# Facile synthesis and electrochemical properties of two trinuclear ruthenium complexes based on star-shaped terpyridine derivatives†

**Cédric R. Mayer,*[a] Frédéric Dumur,[a] Fabien Miomandre,[b] Eddy Dumas,[a] Thomas Devic,[a] Céline Fosse[c] and Francis Sécheresse[a]**

***Received (in Montpellier, France) 27th April 2007, Accepted 13th June 2007***
***First published as an Advance Article on the web 5th July 2007***
**DOI: 10.1039/b706419e**

Two trinuclear ruthenium complexes $[\{Tolyl\text{TerpyRu}\}_3(L3A)]\cdot(PF_6)_9$ and $[\{Tolyl\text{TerpyRu}\}_3(L3B)]\cdot(PF_6)_9$ containing the star-shaped ligands 1,3,5-tris{[4′-(2,2′:6′,2″-terpyridinyl)-1-pyridiniumyl]methylphenyl}benzene (*L3A*) and 2,4,6-tris{[4′-(2,2′:6′,2″-terpyridinyl)-1-pyridiniumyl]methyl}mesitylene (*L3B*), respectively, have been synthesized and characterized using electrospray ionization mass spectrometry, UV-Vis spectroscopy, $^1$H and $^{13}$C NMR spectroscopy. These cationic ligands have been synthesized using a 1,3,5-triphenylbenzene or a mesitylene core and the N-alkylation of the 4′-pyridyl group of 4′-(4-pyridyl)-2,2′:6′,2″-terpyridine (terpy,py). The electrochemical properties of the two trinuclear ruthenium complexes have been compared to analogous dinuclear and mononuclear ruthenium complexes.



## Introduction

Polypyridyl ruthenium complexes have been extensively investigated because of their varied physicochemical properties, leading to a wide range of successful or potential applications such as solar energy conversion, biotechnologies or electroluminescent devices.[1] Hundreds of such complexes have been described due to the ability of chemists to build virtually "on-demand" polypyridyl ligands. Among the variety of *N*-heterocycles, 2,2′-bipyridine and 2,2′:6′,2″-terpyridine (terpy) derivatives have been thoroughly studied. Hosseini and co-workers recently reviewed an exhaustive database of ligands comprising two 2,2′-bipyridine units.[2] The tridentate 2,2′:6′,2″-terpyridine unit has been extensively used to generate original inorganic–organic hybrid structures due to its high affinity toward transition metal ions. For example, the major role of terpy in metallosupramolecular chemistry has been recently examined.[3,4] Another major feature accounting for the tremendous interest in terpy lies in its "facile" 4′-functionalization.[3–7] Among these 4′-functionalized terpy, 4′-(4-pyridyl)-2,2′:6′,2″-terpyridine (terpy,py) has proven to be a versatile heteroditopic ligand for the controlled self-assembly of monolayers of metallic complexes on platinum surface,[8] or to build metallamacrocycles or metallapolymers.[9] The pyridine pendant group of terpy,py can be further modified to synthesize ligands with specific characteristics. For example, we recently used the strong affinity of the 2-mercaptopyridine moiety of the 4′-(2-mercaptopyridyl)-2,2′:6′,2″-terpyridine ligand to stabilize and functionalize gold nanoparticles. The nanocomposites thus generated, bearing terpy pendant groups, have then been used as effective platform for coordination chemistry.[10] Constable *et al.* elegantly used the N-alkylation of the 4′-pyridyl group of terpy,py to isolate metallamacrocycle complexes.[9,11,12] In these supramolecular assemblies, two $\{M(terpy,py)_2\}$ (M = Fe(II), Ru(II)) units were linked through aryl bridges. Inspired by these initial studies, Kurth *et al.* recently reported the synthesis of electrochromic thin films incorporating a new cobalt(II)-metallaviologen.[13]

Our group recently reported the elaboration of nanocomposites in which gold or silver nanoparticles were stabilized and functionalized by polypyridyl ruthenium complexes.[10,14,15] The aim of our studies is to induce a synergistic effect between the intrinsic properties of the two nanocomposite components, namely the metallic nanoparticle and the ruthenium complex. Polypyridyl ruthenium complexes have been chosen due to their extensively studied optical and electrochemical properties. Ru(II) has also been chosen because of its already established ability to generate asymmetric salts of general formula $[RuLL']^{2+}$, *L* and *L′* being tridentate ligands such as terpy derivatives. Up till now, we employed only mononuclear complexes and the next step is indeed the extension to polynuclear ruthenium complexes. In this context, star-shaped polynuclear metallic complexes have been selected due to their attractive physico-chemical properties.[16–18]

In this paper, we took advantage of the facile N-alkylation of the 4′-pyridyl pendant group of terpy,py to synthesize two new tripodal terpy-terminated ligands (Scheme 1, *L3A* and *L3B*) that can further coordinate three Ru(II) centres. Both star-shaped ligands differ by the nature of the core

[a] *Institut Lavoisier de Versailles, UMR 8180, Université de Versailles, 45 Avenue des Etats-Unis, 78035 Versailles, France. E-mail: cmayer@chimie.uvsq.fr; Fax: +33 1 39 25 43 81; Tel: +33 1 39 25 43 97*
[b] *Laboratoire PPSM, UMR 8531, Ecole Normale Supérieure de Cachan, 61 Avenue du Président Wilson, 94235 Cachan, France*
[c] *Service de Spectrométrie de Masse, Ecole Nationale Supérieure de Chimie de Paris, 24 Rue Lhomond, 75231 Paris Cedex 05, France*
† Electronic supplementary information (ESI) available: $^{13}$C NMR spectra of *L3B* and *Ru3B*. Plot of peak current *vs.* square root of the scan rate for compounds *Ru1*, *Ru2* and *Ru3A*. See DOI: 10.1039/b706419e

 

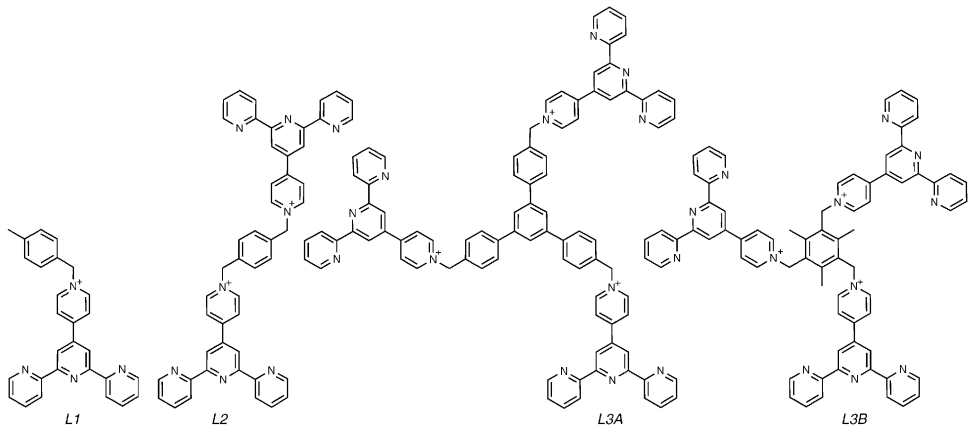


**Scheme 1** Structures of the ligands used in this paper.



(1,3,5-triphenylbenzene or mesitylene) and by the presence of an additional phenylene group in each arm of the spacer connected to the three terpy pendant groups. Here, we report the syntheses and the characterization ($^{1}$H and $^{13}$C NMR, ESI-MS, UV/Vis) of the two aforementioned ligands and of the corresponding triruthenium complexes. To discuss the electrochemical properties of the two trinuclear ruthenium complexes *Ru3A* and *Ru3B*, analogous dinuclear (*Ru2*) and mononuclear (*Ru1*) ruthenium complexes have been synthesized and characterized.

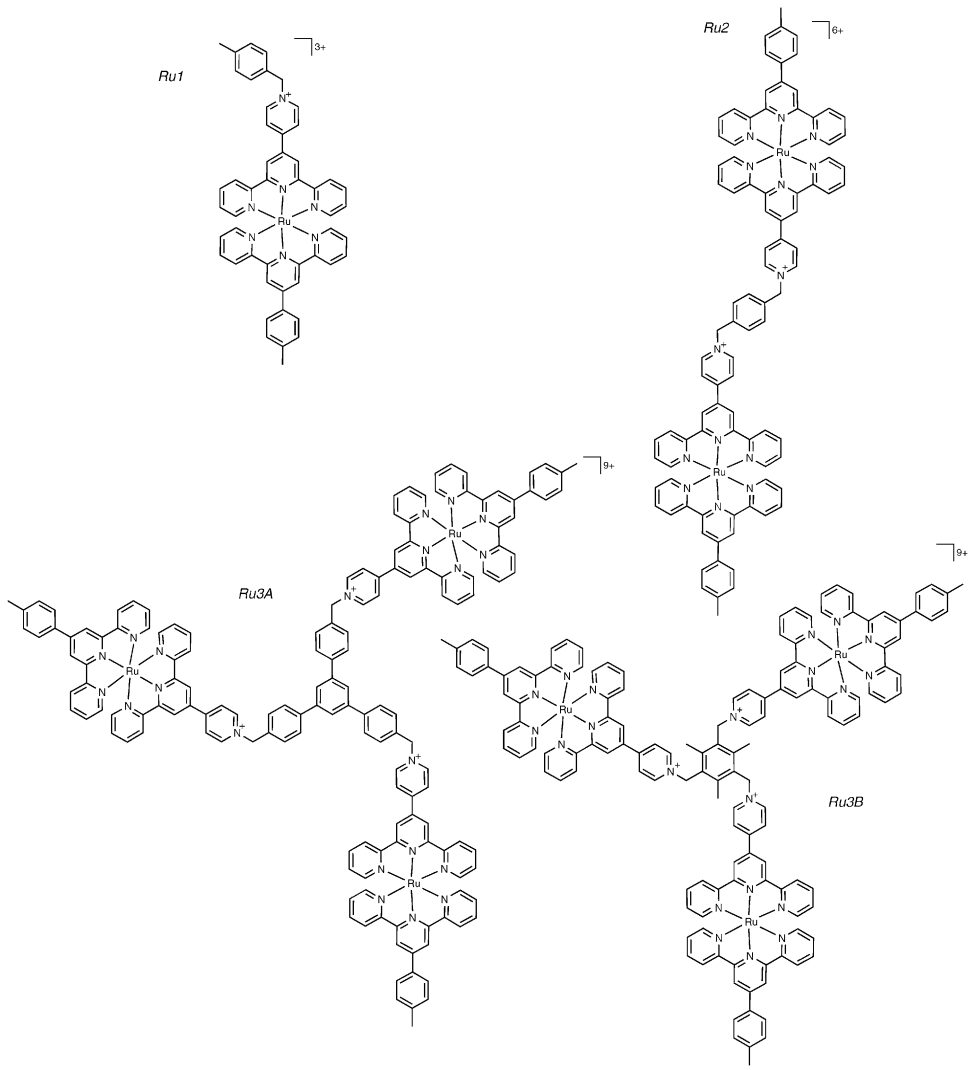


**Scheme 2** Structures of the ruthenium complexes reported in this paper.

## Results and discussion

### Syntheses of ligands and ruthenium complexes

Star-shaped ligands have been synthesized using a variety of cores such as nitrogen atom,[19] benzene substituted in 1,3,5 positions[16] or 1,3,5-triazine substituted in 2,4,6 positions.[16,20] In this paper, ligands were obtained by using a benzene derivative core and the N-alkylation of the 4′-pyridyl group of terpy,py.

Ligand *L3A* (Scheme 1) was obtained starting from 1,3,5-tris[4-methylphenyl]benzene that was reacted with three equivalents of NBS to give 1,3,5-tris[4-(bromomethyl)phenyl]-benzene. The later was finally converted to *L3A* by reaction with three equivalents of terpy,py. Ligands *L3B* and *L1* (Scheme 1) were synthesized following the procedure described for *L*3A but starting from the commercially available 2,4,6-tris(bromomethyl)mesitylene, and 4-bromomethyltoluene, respectively. The four ligands *L3A*, *L3B*, *L2*[13] and *L1* were reacted with three, three, two and one equivalent(s) of [{4′-(4-tolyl)-2,2′,6′,2″-terpyridine}$RuCl_3$] (*Tolyl*TerpyRu$Cl_3$), respectively, in a refluxing mixture of EtOH–$H_2O$–DMF to give the ruthenium complexes *Ru3A*, *Ru3B*, *Ru2* and *Ru1* (Scheme 2).

### Electrospray ionization mass spectrometry, $^1$H and $^{13}$C NMR

Two types of mass spectrometers were used to characterize the ligands and the ruthenium complexes described in this article. The single quadrupole mass spectrometer allowed the characterization of the ligands but not the identification of the final ruthenium complexes. A systematic fragmentation of the ruthenium complexes was detected and only two peaks were observed at $m/z$ = *ca.* 367.6 and 880.1, attributed to $[(Tolyl\text{-Terpy})Ru(terpy,py)]^{2+}$ and $[(Tolyl\text{Terpy})Ru(terpy,py) + PF_6]^+$, respectively. Consequently, *Ru3A*, *Ru3B*, *Ru2* and *Ru1* were characterized using the triple quadrupole mass spectrometer. The resolution of the peak at $m/z$ = 1140.2 attributed to $[\{(Tolyl\text{Terpy})Ru\}_3(L3A) + 6PF_6]^{3+}$ in the ESI-MS spectrum of *Ru3A* (positive ion mode) is shown in Fig. 1(a) (measured) and (b) (calculated). The ESI-MS spectrum (positive ion mode) of *Ru3B* is shown in Fig. 1(c). Two peaks attributed to the fragmentation of this trinuclear complex were still observed at $m/z$ = 367.9 and 880.6 (marked with an asterisk in Fig. 1) but six other peaks were detected on the spectrum. These six peaks were straightforwardly attributed to the six different states of charge ($z$) corresponding to the ion pairs of general formula $[\{(Tolyl\text{Terpy})Ru\}_3(L3B) + xPF_6]^{z+}$, with $z = 9 - x$ and $1 \leq x \leq 6$. For all these peaks, the envelope of the isotopic pattern was in good agreement with the simulated ones.

The $^1$H and $^{13}$C NMR spectra were recorded in DMSO-$d_6$. A complete assignment of the $^1$H (Fig. 2) and $^{13}$C NMR spectra of *L3B* and *Ru3B* was realized by using two-dimensional COSY and HMQC experiments (Fig. 3). Characteristic features were obtained from these spectra. For example, the N-alkylation of the three 4′-pyridyl pendant groups was evidenced by the presence of a single peak at $\delta$ = 6.28 ppm assigned to $H_4$ ($^+NCH_2$ group) in the $^1$H NMR spectrum of *L3B*. Identical assignments were realized for $\delta$ 6, 5.95 and 5.89 ppm for *L3A*, *L2* and *L1*, respectively. The N-alkylation was also confirmed by the set of peaks located between 7 and 10 ppm attributed to the aromatic protons, characteristic of a symmetrical complex, and by the integration of these aromatic protons compared with the integration of the protons $H_4$ (see above) and $H_1$ (–$CH_3$, $\delta$ 2.59 ppm) of the central mesitylene derivative. The N-alkylation also induced a noticeable downfield shift of the protons of the pyridyl group ($H_5$ and $H_6$). The reaction of *Tolyl*TerpyRu$Cl_3$ with *L3B* was indeed corroborated by significant chemical shifts of the protons of the pendant terpy group of *L3B* (for example, $\Delta\delta$ = −1.28 ppm for $H_{15}$).

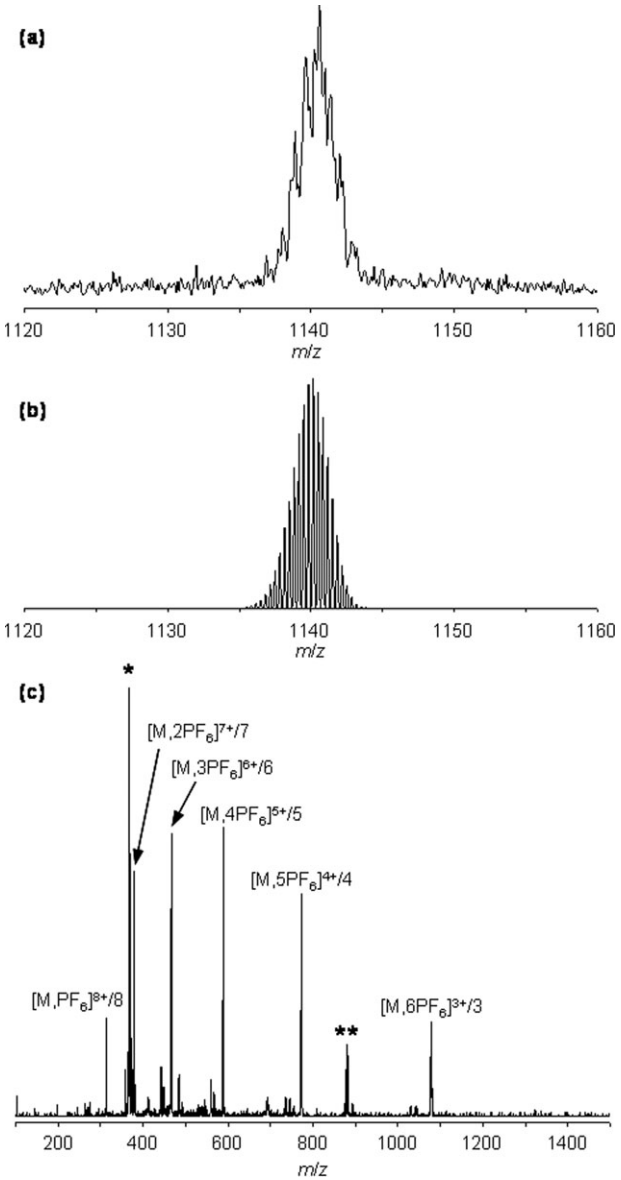


**Fig. 1** Resolution of the peak at $m/z$ = 1140.6 attributed to $[\{(Tolyl\text{Terpy})Ru\}_3(L3A) + 6PF_6]^{3+}$ in the ESI-MS spectrum of *Ru3A*, (a) measured and (b) calculated. (c) ESI-MS spectrum of *Ru3B* (see text). Peaks marked with * and ** are attributed to $[(Tolyl\text{Terpy})Ru(terpy,py)]^{2+}$ and $[(Tolyl\text{Terpy})Ru(terpy,py) + PF_6]^+$, respectively.

 

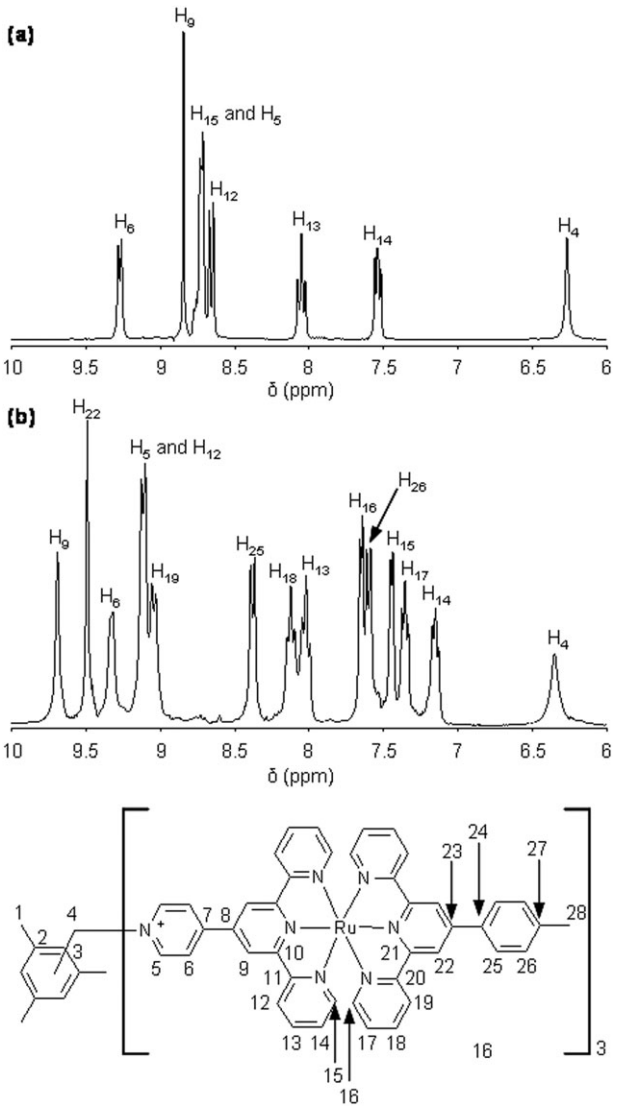


**Fig. 2** $^{1}$H NMR spectra of (a) *L3B* and (b) *Ru3B*.

Other ligands and ruthenium complexes reported in this article were also characterized using ESI-MS, $^{1}$H and $^{13}$C NMR spectroscopy. The $^{1}$H NMR spectrum of *Ru3A* is shown in Fig. 4.

## Electrochemistry

The electrochemical properties of *Ru3A*, *Ru3B*, *Ru2* and *Ru1* were investigated in acetonitrile on platinum electrode. Typical cyclic voltammograms (CVs) are shown in Fig. 5, in the case of *Ru1* (Fig. 5(a)) and *Ru3A* (Fig. 5(b)). Four reversible redox waves can be clearly identified for each compound. The values of the standard potentials associated to these redox couples are listed in Table 1. The oxidation of Ru(II) into Ru(III) occurs at an average standard potential of *ca.* +0.98 V *vs.* $Ag^{+}/Ag$, that is +0.90 V *vs.* $Fc^{+}/Fc$, which is very close to the standard potential for $Ru(tpy)_2^{2+}$.[21] This result evidences that oxidation is fully centred on Ru, with very weak influence of the ligand nature. This is also confirmed by the comparison with two similar complexes of *Ru1*, namely those in which the tolylpyridinium moiety is replaced by a pyridine (*Ru1′*) or a 2-chloropyridine (*Ru1″*). This comparison between three mononuclear complexes is also useful to assess the reduction waves: the most cathodic redox couple clearly involves the reduction of the tolyl substituted terpy, which is the electron richest ligand: its standard potential lies in the same range as the lowest one in $[Ru(tpy)_2]^{2+}$, despite the donor character of the tolyl group, counter-balanced by the electroattracting substituents on the other tpy. The intermediate redox system is present in all the *Ru1*, *Ru1′* and *Ru1″* complexes, thus involving the pyridinium substituted terpy ligand. The standard potential is positively shifted by *ca.* 130 mV *vs.* tpy due to the electron withdrawal effect (although the now reduced pyridinium function alleviates this effect). However this shift is stronger than for pyridine substitution, as was already mentioned by Constable *et al.*[22] It is noteworthy that this redox system presents marked adsorption features, especially in the case of *Ru3A*. Finally the least cathodic peak corresponds to the reduction of the tolylpyridinium into a stable radical (note that all these reduction waves correspond to monoelectronic transfers, as evidenced by the comparison between peak

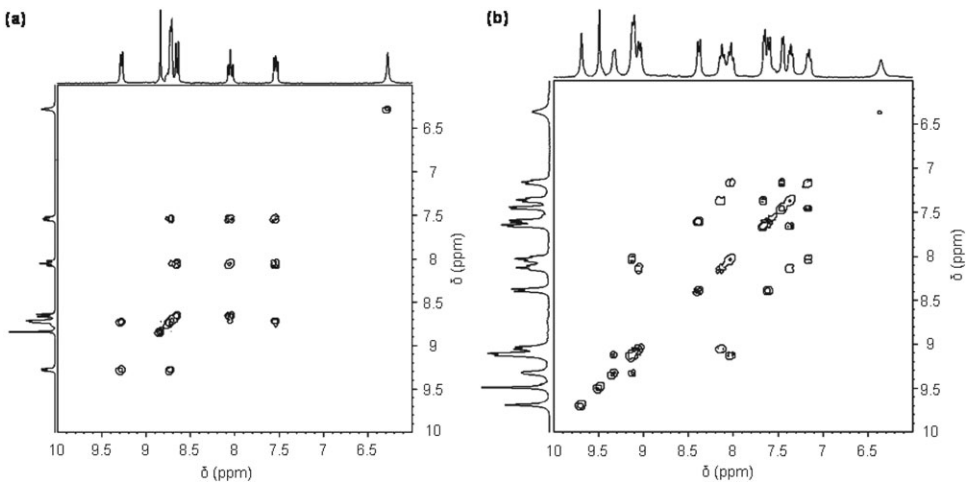


**Fig. 3** COSY spectra of (a) *L3B* and (b) *Ru3B*.

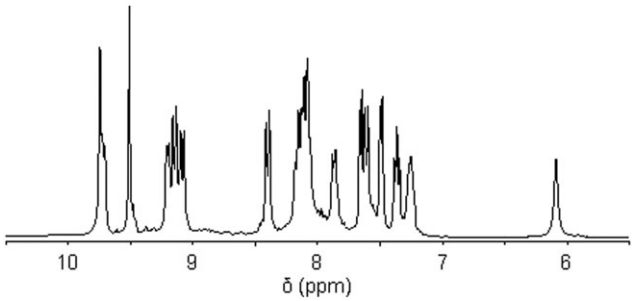


**Fig. 4** $^{1}$H NMR spectrum of *Ru3a*.

currents): this reduction is reversible, demonstrating the highly delocalized nature of the formed radical, compared to general alkylpyridinium compounds;[23] it occurs at relatively high potentials, actually only 100 to 150 mV more negative than the reduction of the same function in methylpyridiniumtris-pyridylpyrazine (see Table 1), the difference being due to the higher attracting power of pyrazine compared to pyridine group.

Table 1 also summarizes the comparison between standard potential values for mononuclear (*Ru1*), dinuclear (*Ru2*) and trinuclear (*Ru3A* and *Ru3B*) compounds. With the exception of the first reduction of *Ru3B*, one can notice the quasi-invariance of all these potentials with the number of Ru atoms in the complex, as an evidence of the absence of interactions between redox centres. This result was expected due to the interrupted conjugation induced by the methyl group connecting the terpy,py and the core of the complex and also due to the large distance between metallic centres in the case of the oxidation waves. In the case of *Ru3B*, the first reduction potential is shifted positively, as a result of stronger coulombic repulsion between pyridinium groups within this complex compared to the analogous *Ru3A*, making it easier to reduce. It is also worth mentioning that the peak to peak separation for the oxidation of *Ru1* and *Ru3A* is nearly the same, which is an evidence for the same number of electrons exchanged (namely one) during the rate determining step of the charge transfer kinetics: thus the three electrons in *Ru3A* are withdrawn at the same potential but not at the same rate, as is usually the case in multielectronic systems.[23]

Besides the determination of thermodynamic potentials, CVs recorded at various scan rates can also give valuable information about the diffusion features of all these compounds. The plot of the anodic peak current (A) *vs.* the square root of scan rate (V s$^{-1}$) for Ru(II)/Ru(III) leads to straight lines (see ESI†), with slopes given by the Randles–Sevčik equation:[25]

$$i_p = (2.7 \times 10^5) nAC\sqrt{D}\sqrt{v}$$

with: $n$ = total number of exchanged electrons
$A$ = electroactive area of the electrode (cm$^2$)
$C$ = bulk concentration of the electroactive species (mol cm$^{-3}$)
$D$ = diffusion coefficient (cm$^2$ s$^{-1}$)

Recording the same curve $I_p$ *vs.* $v^{1/2}$ for a standard compound like ferrocene ($D_{Fc} = 2.3 \times 10^{-5}$ cm$^2$ s$^{-1}$ in acetonitrile)[26] in the same experimental conditions allows us to get rid of the unknown $A$ factor, thus giving values for the product

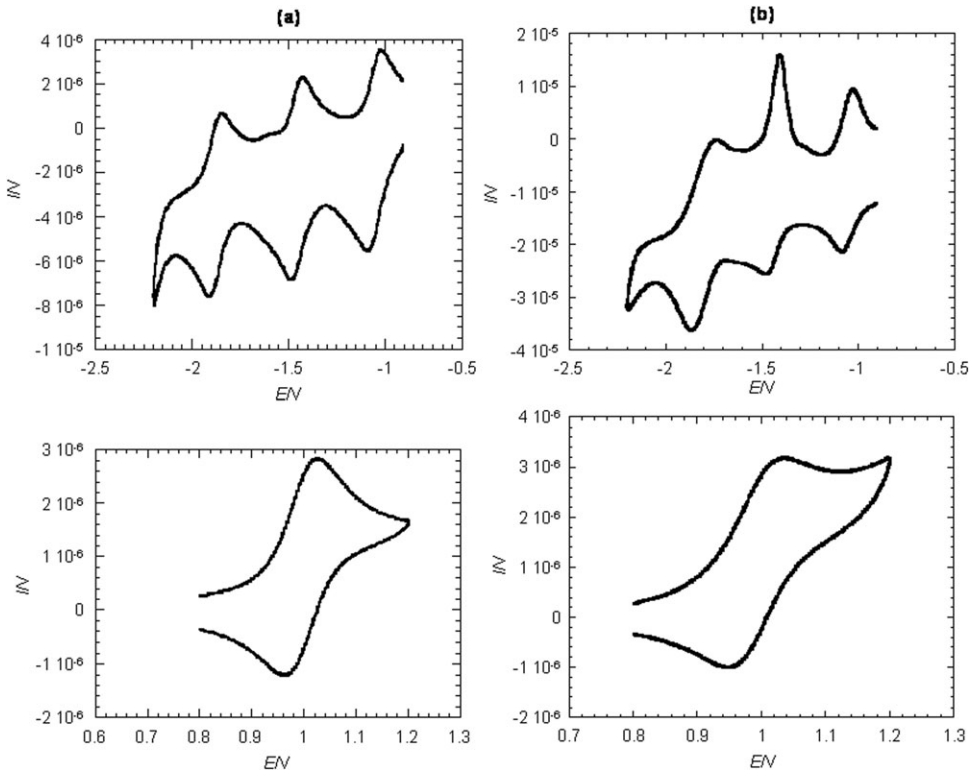


**Fig. 5** CVs (cathodic part upwards and anodic part downwards) of: (a) *Ru1* (*ca.* $8 \times 10^{-4}$ M) and (b) *Ru3A* (*ca.* $2 \times 10^{-4}$ M) in acetonitrile + $TBAPF_6$ on Pt electrode. Scan rate: 200 mV s$^{-1}$. Potentials refer to $Ag^+$/Ag reference electrode.

 

**Table 1** Electrochemical data for compounds *Ru1*, *Ru2*, *Ru3A* and *Ru3B* and similar compounds. Compounds *Ru1′* and *Ru1″* are the analogues of *Ru1* by substituting the tolylpyridinium moiety by, respectively pyridine and 2-chloropyridine at the same position. *Tpy* = terpyridine; *Metpp* = 2-[2-(1-methylpyridinium)]-3,5,6-tri(2-pyridyl)pyrazine. Potential values refer to ferrocene (+0.08 V *vs.* our reference)

| Compound | $E^{\circ}_{ox}$/V | $\Delta E_p$/mV | $E^{\circ}_{red\ 1}$/V | $\Delta E_p$/mV | $E^{\circ}_{red\ 2}$/V | $\Delta E_p$/mV | $E^{\circ}_{red\ 3}$/V | $\Delta E_p$/mV |
|---|---|---|---|---|---|---|---|---|
| *Ru1* | 0.91 | 68 | −1.10 | 65 | −1.51 | 65 | −1.93 | 100 |
| *Ru1′* | 0.87 | 55 | — | — | −1.61[a] | — | −1.89[a] | — |
| *Ru1″* | 0.88 | 70 | — | — | −1.56[a] | — | −1.89[a] | — |
| *Ru2* | 0.89 | 60 | −1.12 | 60 | −1.52 | 60 | −1.86 | 140 |
| *Ru3A* | 0.89 | 78 | −1.13 | 70 | −1.52 | 76 | −1.87 | 140 |
| *Ru3B* | 0.93 | 85 | −1.07[a] | — | −1.53[a] | — | −1.87[a] | — |
| $Ru(tpy)_2^{2+}$ | 0.88[b] | — | | | −1.65[b] | | −1.90[b] | |
| $Ru(tpy)(Metpy)^{3+}$ | 1.20[c] | — | −1.00[c] | — | −1.15[c] | — | −1.95[c] | — |

[a] Peak potentials. [b] From ref. 20. [c] From ref. 24.



$nD^{1/2}$. The values of $D$ deduced from the slopes for the four complexes are given in Table 2, assuming that the number of exchanged electrons is equal to the number of ruthenium centres. These values range well with the variation of size when the number or ruthenium centres increases. In particular, one can consider that the radius of *Ru3A* is approximately equal to the diameter of *Ru1*, since this latter constitutes one "arm" of the tripodal trinuclear complex. Thus one can expect that the diffusion coefficient of *Ru3A* to be around one half of that of *Ru1*, based on Stokes–Einstein relationship. In the case of *Ru2*, the diffusion coefficient value is found closer to that of *Ru1*, probably because of the anisotropy of this complex that has a cylindrical shape rather than a spherical one for the two others. The good agreement between the measured values of the diffusion coefficient and the geometries of the complexes validates the assumption concerning the number of exchanged electrons per ruthenium centre, as also confirmed by the comparison of the current peaks between oxidation of ruthenium and reduction of the ligand in each compound.

### UV-Vis spectroscopy

Absorption spectra were recorded for complexes *Ru3A*, *Ru3B*, *Ru2* and *Ru1* in acetonitrile and show the classical features for this kind of coordination compounds,[22] especially the presence of a broad MLCT absorption band in the 500 nm wavelength region. The position of the MLCT absorption band is red shifted by *ca.* 25 nm compared to $Ru(tpy)^{2+}$, which seems in agreement with the less negative reduction potential of the pyridinium substituted tpy ligand, resulting in a stabilized LUMO.

The maximum absorption wavelength is independent of the number of ruthenium centres, confirming the absence of interactions predicted by the electrochemical results. The molar extinction coefficient values for this MLCT band increases with the number of Ru centres (see Table 3), in accordance with an increasing number of chromophores, but not strictly proportionally to that number, possibly because of a partial overlap between the absorption cross sections of each chromophore.

Finally, one can mention that these complexes are almost not luminescent at room temperature, as expected for tpy substituted ruthenium complexes although in some cases, the modification or substitution of the tpy ligand can induce enhanced luminescence properties.[27]

**Table 2** Diffusion coefficients for compounds *Ru1*, *Ru2* and *Ru3A*, deduced from the slopes of $i_p$ *vs.* $v^{1/2}$ for the oxidation of Ru(II), assuming one exchanged electron per ruthenium centre

| Compound | $D/10^{-5}$ cm$^2$ s$^{-1}$ |
|---|---|
| *Ru1* | 0.93 |
| *Ru2* | 0.86 |
| *Ru3A* | 0.51 |

## Conclusions

N-alkylation of the 4′-pyridyl group of 4′-(4-pyridyl)-2,2′:6′,2″-terpyridine (terpy,py) using tribromo-benzene or -mesitylene derivative cores has been efficiently used to generate original star-shaped ligands bearing three terpyridine pendant groups. Such tripodal ligands can straightforwardly react with metal complexes such as [(4′-functionalized-terpy)$RuCl_3$]. Two trinuclear ruthenium complexes have been synthesized and characterized in this paper but the construction of star-shaped metallodendrimers can also be foreseen. In addition, the introduction of specific pendant groups such as thiol or mercaptopyridine would generate supramolecular complexes adapted for the functionalization of metallic nanoparticles. Such polynuclear multifunctionalized systems are also perfectly adapted for the self-assembly of metallic NPs through reversible redox systems. The well-known acceptor properties of alkylpyridinium groups present in these complexes makes them attractive systems to build multifunctional nanocomposites. The good reversibility of the electrochemical response of these compounds is an essential point to design nanocomposites acting as redox probes, sensitive to their environment; this is also a key feature to investigate the influence of the nanoparticle on the electrochemical properties of the coordination complex in the nanocomposite.

**Table 3** Maximum absorption wavelength and molar extinction coefficient for solutions of *Ru1*, *Ru2*, *Ru3A* and *Ru3B* in acetonitrile (the concentration in complex ranges from $4 \times 10^{-6}$ M to $1.4 \times 10^{-5}$ M for Beer–Lambert plots)

| Compound | $\lambda_{max}$/nm | $\varepsilon/10^4$ L mol$^{-1}$ cm$^{-1}$ |
|---|---|---|
| *Ru1* | 503 | 3.09 |
| *Ru2* | 500 | 4.61 |
| *Ru3A* | 498 | 6.56 |
| *Ru3B* | 505 | 6.50 |

## Experimental

### General methods

ESI-MS measurements were carried out with an API 3000 (ESI/MS/MS) PE-SCIEX triple quadrupole mass spectrometer and HP 5989B single quadrupole mass spectrometer equipped with an electrospray source from Analytica of Branford. Both instruments were operated in the positive ion mode. For the API 3000 (ESI/MS/MS) PE SCIEX triple quadrupole mass spectrometer, the experiments were performed either by direct infusion with a syringe pump with flow rate of 10 μL $min^{-1}$ or flow injection acquisition with flow rate of 200 μL $min^{-1}$. Standard experimental conditions were as follows: sample concentration $10^{-3}$ to $10^{-5}$ M, nebulizing gas $N_2$: 7 units flow rate, ion spray voltage −5.00 kV, temperature: 200–400 °C, declustering potential: −20 V, focusing potential: −200 V, entrance potential: 10 V.

UV-Vis spectra were recorded using a CARY 500 UV-Vis-NIR spectrophotometer (Varian). Each sample was analyzed in a similar way: about 10 μL of a 1 mM solution of the complex were introduced into the cell (1 cm optical path) and diluted with an appropriate volume of acetonitrile (spectroscopic grade), in order to obtain absorbance values lower than 1. Measurements of the molar absorption coefficient were made by recording the spectra corresponding to several aliquots of 10 μL of the complex solution in 2 mL of acetonitrile, and then drawing a Beer–Lambert plot.

$^1H$ and $^{13}C$ NMR spectra were obtained at room temperature in 5 mm o.d. tubes on a Bruker Avance 300 spectrometer equipped with a QNP probe head. A numbering scheme of the ligands and complexes is given in ESI† when needed for the assignment.

Electrochemical measurements were performed in a three-electrode cell equipped with a 1 mm diameter platinum disk as the working electrode, platinum wire as the counter electrode and $Ag^+$(0.01 M)/Ag as the reference electrode. The reference potential was checked *vs.* ferrocene as recommended by IUPAC ($E^\circ_{Fc}$ = +86 mV). The supporting electrolyte was tetrabutylammonium hexafluorophosphate (Fluka, puriss.) and the solutions were deaerated by argon bubbling prior each experiment. Cyclic voltammograms (CVs) were recorded with a 600 CHInstruments potentiostat connected to a PC.

### Syntheses

All starting materials and solvents were purchased from Aldrich Chemical Company and used without further purification. 4′-(4-pyridyl)-2,2′:6′,2″-terpyridine (terpy,py),[28] 1,3,5-tris[4-methylphenyl]benzene,[29] 1,3,5-tris[4-(bromomethyl)phenyl]benzene,[30] 1,4-bis{[4′-(2,2′:6′,2″-terpyridinyl)-1-pyridiniumyl]methyl}benzene dibromide (*L2*),[13] 4′-(4-tolyl)-2,2′,6′,2″-terpyridine (*Tolyl*Terpy) and *Tolyl*TerpyRu$Cl_3$,[31] were synthesized following the procedures previously reported without modification.

**1,3,5-Tris{[4′-(2,2′:6′,2″-terpyridinyl)-1-pyridiniumyl]methylphenyl}benzene tribromide (*L3A*·$Br_3$).** terpy,py (95 mg, 0.31 mmol) and 1,3,5-tris[4-(bromomethyl)phenyl]benzene (59 mg, 0.10 mmol) were suspended in acetonitrile (70 mL). 0.5 h at reflux was needed to solubilize both reagents. The resulting solution was then maintained at reflux overnight, leading to the precipitation of a white solid. The reaction mixture was cooled to room temperature. The white precipitate was filtered off, washed with dichloromethane (20 mL), diethyl ether (20 mL) and dried under vacuum to afford *L3A*·$Br_3$ in 86% yield (Found: C, 68.7; H, 4.0; Br, 15.6; N, 10.9. $C_{87}H_{63}Br_3N_{12}$ requires C, 68.9; H, 4.2; Br, 15.8; N, 11.1%); $\delta_H$ (300 MHz; DMSO-$d_6$; $Me_4Si$; 25 °C) 6.0 (6H, br s), 7.6 (6H, dd), 7.77 (6H, dd), 8.0 (6H, td), 8.1 (6H, td), 8.71 (6H, td), 8.77 (3H, s), 8.79 (6H, d), 8.85 (6H, d), 8.91 (6H, s) and 9.45 (2H, d); *m*/*z* (ESI-MS, HP 5989B) 425.1 ($M^{3+}$ requires 425.5).

**2,4,6-Tris{[4′-(2,2′:6′,2″-terpyridinyl)-1-pyridiniumyl]methyl}-mesitylene tribromide (*L3B*·$Br_3$).** *L3B*·$Br_3$ was synthesized from terpy,py (95 mg, 0.31 mmol) and 2,4,6-tris(bromomethyl)mesitylene (39.9 mg, 0.10 mmol), using the procedure described for the synthesis of *L3A*·$Br_3$, in 83% yield (Found: C, 64.7; H, 4.4; Br, 18.4; N, 12.3. $C_{72}H_{57}Br_3N_{12}$ requires C, 65.0; H, 4.3; Br, 18.0; N, 12.6%); $\delta_H$ (300 MHz; DMSO-$d_6$; $Me_4Si$; 25 °C) 2.43 (9H, s, $H_1$), 6.28 (6H, br s, $H_4$), 7.54 (6H, dd, $^3J$ = 7.2 Hz, $^3J'$ = 6.9 Hz, $H_{14}$), 8.06 (6H, td, $^3J_{13-12}$ = $^3J_{13-14}$ = 7.8 Hz, $^4J_{13-15}$ = 1.5 Hz, $H_{13}$), 8.65 (4H, d, $^3J_{12-13}$ = 7.8 Hz, $H_{12}$), 8.70–8.76 (10H, m, $H_{15}$ and $H_5$), 8.84 (6H, s, $H_9$) and 9.28 (6H, d, $^3J_{5-6}$ = 6.5 Hz, $H_6$); $\delta_C$ (75 MHz; DMSO-$d_6$; $Me_4Si$; 25 °C) 16.9 ($C_1$), 58.1 ($C_4$), 118.02 ($C_9$), 121.0 ($C_{12}$), 124.7 ($C_{14}$), 126.2 ($C_5$), 128.9 ($C_2$), 137.6 ($C_{13}$), 143.7 ($C_3$), 143.8 ($C_8$), 144.8 ($C_6$), 149.4 ($C_{15}$), 152.8 ($C_7$), 154.0 ($C_{11}$) and 156.3 ($C_{10}$); *m*/*z* (ESI-MS, API 3000) 363.5 ($M^{3+}$ requires 363.4), 585.6 ($[M + Br]^{2+}$ requires 585.1) and 1249.9 ($[M + 2Br]^+$ requires 1250.1).

**4-{[4′-(2,2′:6′,2″-Terpyridinyl)-1-pyridiniumyl]methyl}toluene bromide (*L1*·Br).** *L1*·Br was obtained from terpy,py (31 mg, 0.10 mmol) and 4-bromomethyltoluene (49.5 mg, 0.10 mmol) following the procedure described for the synthesis of *L3A*·$Br_3$, in 82% yield (Found: C, 67.1; H, 4.5; Br, 16.5; N, 11.1. $C_{28}H_{23}BrN_4$ requires C, 67.9; H, 4.7; Br, 16.1; N, 11.3%); $\delta_H$ (300 MHz; DMSO-$d_6$; $Me_4Si$; 25 °C) 2.32 (3H, s), 5.89 (2H, br s), 7.29 (2H, d), 7.5 (2H, d), 7.59 (2H, td), 8.1 (2H, td), 8.71 (2H, d), 8.77–8.81 (4H, m), 8.90 (2H, s), 9.34 (2H, d); *m*/*z* (ESI-MS, HP 5989B) 415.6 ($M^+$ requires 415.5).

**[{*Tolyl*TerpyRu}$_3$(*L3A*)]·$(PF_6)_9$ (*Ru3A*·$(PF_6)_9$).** *Tolyl*TerpyRu$Cl_3$ (53.1 mg, 0.10 mmol) and *L3A*·$Br_3$ (50 mg, 3.3 $10^{-2}$ mmol) were refluxed overnight in a mixture of EtOH–$H_2O$–DMF (30 : 20 : 1 mL). The mixture was then cooled to room temperature and an aqueous solution of $NH_4PF_6$ (200 mg, 5 mL) was added. The resulting mixture was concentrated under vacuum to *ca.* 25 mL and 60 mL of water were added. The red solid obtained was filtered off and washed with ethanol (3 × 10 mL) and diethyl ether (3 × 10 mL). *Ru3A*·$(PF_6)_9$ was recrystallized from acetonitrile, by diffusion of diethyl ether, in 71% yield (Found: C, 46.9; H, 2.8; F, 27.4; N, 7.2; P, 8.0; Ru, 7.7. $C_{153}H_{114}F_{54}N_{21}P_9Ru_3$ requires C, 47.7; H, 3.0; F, 26.6; N, 7.6; P, 7.2; Ru, 7.9%); $\delta_H$ (300 MHz; DMSO-$d_6$; $Me_4Si$; 25 °C) 2.53 (9H, s, $H_{31}$), 6.10 (6H, br s, $H_7$), 7.22–7.28 (6H, m), 7.36 (6H, t, *J* = 6.6 Hz), 7.49 (6H, d, *J* = 5.5 Hz), 7.60 (6H, d, *J* = 8.0 Hz), 7.65 (6H, d, *J* = 5.5 Hz), 7.84–7.88 (6H, m), 8.06–8.18 (22H, m), 8.39 (6H, d, *J* = 7.2 Hz), 9.07–9.21 (18H, m), 9.51 (6H, s), 9.70–9.75

 

(11H, m); $\delta_C$ (75 MHz; DMSO-$d_6$; $Me_4Si$; 25 °C) 20.7, 20.9, 30.6, 35.7, 38.6, 38.9, 39.2, 39.5, 39.7, 40.0, 40.3, 63.0, 120.9, 122.0, 124.9, 125.0, 125.8, 127.0, 127.6, 128.1, 129.5, 130.0, 130.1, 133.0, 133.9, 138.2, 138.3, 138.9, 140.5, 140.8, 140.9, 145.7, 147.7, 151.8, 152.2, 152.3, 154.5, 155.0, 155.9, 157.5, 157.9; *m*/*z* (ESI-MS, API 3000) 283.6 ($[M + PF_6]^{8+}$ requires 283.4), 337.2 ($[M + 2PF_6]^{7+}$ requires 337.0), 497.9 ($[M + 3PF_6]^{6+}$ requires 497.6), 626.7 ($[M + 4PF_6]^{5+}$ requires 626.1), 819.0 ($[M + 5PF_6]^{4+}$ requires 818.9), 1140.6 ($[M + 6PF_6]^{3+}$ requires 1140.2).

**[{*Tolyl*TerpyRu}$_3$(*L3B*)]·(PF$_6$)$_9$ (*Ru3B*·(PF$_6$)$_9$).** *Ru3B*·$(PF_6)_9$ was synthesized by the reaction of *Tolyl*TerpyRuCl$_3$ (53.1 mg, 0.10 mmol) and *L3B*·Br$_3$ (44 mg, $3.3 \times 10^{-2}$ mmol), using the procedure described for the synthesis of *Ru3A*·$(PF_6)_9$, in 73% yield (Found: C, 44.6; H, 3.3; F, 29.2; N, 7.7; P, 7.9; Ru, 8.0. $C_{138}H_{108}F_{54}N_{21}P_9Ru_3$ requires C, 45.2; H, 3.0; F, 28.0; N, 8.0; P, 7.6; Ru, 8.3%); $\delta_H$ (300 MHz; DMSO-$d_6$; $Me_4Si$; 25 °C) 2.53 (9H, s, $H_{28}$), 2.59 (9H, s, $H_1$), 6.36 (6H, br s, $H_4$), 7.15 (6H, t, $^3J$ = 6.7 Hz, $H_{14}$), 7.36 (6H, t, $^3J$ = 6.3 Hz, $H_{17}$), 7.45 (6H, d, $^3J$ = 6.7 Hz, $H_{15}$), 7.60 (6H, d, $^3J$ = 8.1 Hz, $H_{26}$), 7.65 (6H, d, $^3J$ = 5.1 Hz, $H_{16}$), 8.03 (6H, t, $^3J$ = 7.8 Hz, $H_{13}$), 8.13 (6H, t, $^3J$ = 6.9 Hz, $H_{18}$), 8.38 (6H, d, $^3J$ = 8.1 Hz, $H_{25}$), 9.04 (6H, d, $^3J$ = 6.9 Hz, $H_{19}$), 9.08–9.15 (12H, m, $H_5$ and $H_{12}$), 9.33 (6H, d, $^3J_{6-5}$ = 4.9 Hz, $H_6$), 9.49 (6H, s, $H_{22}$ or $H_9$), 9.69 (6H, s, $H_{22}$ or $H_9$); $\delta_C$ (75 MHz; DMSO-$d_6$; $Me_4Si$; 25 °C) 17.0 ($C_1$), 20.9 ($C_{28}$), 56.0 ($C_4$), 120.9 ($C_9$ or $C_{22}$), 122.1 ($C_9$ or $C_{22}$), 123.3 ($C_{27}$ or $C_{10}$), 123.5 ($C_{27}$ or $C_{10}$), 124.8 ($C_5$ or $C_{12}$), 124.9 ($C_{19}$), 125.9 ($C_5$ or $C_{12}$), 127.6 ($C_{25}$), 128.2 ($C_{14}$), 129.1 ($C_{17}$), 130.0 ($C_{26}$), 132.9 ($C_2$), 138.2 ($C_{18}$), 138.3 ($C_{13}$), 139.1 ($C_7$), 140.5 ($C_{24}$), 144.0 ($C_3$), 144.3 ($C_6$), 147.7 ($C_{23}$), 152.1 ($C_{16}$), 152.4 ($C_{15}$), 154.5 ($C_{21}$ or $C_8$), 155.9 ($C_{21}$ or $C_8$), 157.4 ($C_{20}$), 157.9 ($C_{11}$); *m*/*z* (ESI-MS, API 3000) 313.9 ($[M + PF_6]^{8+}$ requires 313.7), 379.6 ($[M + 2PF_6]^{7+}$ requires 379.1), 467.0 ($[M + 3PF_6]^{6+}$ requires 466.4), 588.8 ($[M + 4PF_6]^{5+}$ requires 588.7), 772.7 ($[M + 5PF_6]^{4+}$ requires 772.1), 1078.5 ($[M + 6PF_6]^{3+}$ requires 1077.8).

**[{*Tolyl*TerpyRu}$_2$(*L2*)]·(PF$_6$)$_6$ (*Ru2*·(PF$_6$)$_6$).** *Ru2*·$(PF_6)_6$ was obtained from *Tolyl*TerpyRuCl$_3$ (53.1 mg, 0.10 mmol) and *L2*·Br$_2$ (44 mg, $5 \times 10^{-2}$ mmol) following the procedure described for the synthesis of *Ru3A*·$(PF_6)_9$, in 71% yield (Found: C, 45.6; H, 3.1; F, 28.5; N, 8.2; P, 7.9; Ru, 8.7. $C_{92}H_{70}F_{36}N_{14}P_6Ru_2$ requires C, 45.2; H, 2.9; F, 28.0; N, 8.0; P, 7.6; Ru, 8.3%); $\delta_H$ (300 MHz; DMSO-$d_6$; $Me_4Si$; 25 °C) 2.53 (6H, s), 6.00–6.07 (4H, br s, $H_{12}$), 7.23 (4H, q, $J$ = 6.1 Hz), 7.36 (4H, t, $J$ = 6.2 Hz), 7.47–7.50 (6H, m), 7.60–7.67 (10H, m), 7.84 (2H, s), 8.04–8.18 (8H, m), 8.39 (4H, d, $J$ = 8.1 Hz), 9.07–9.21 (12H, m), 9.50 (4H, s), 9.61–9.67 (4H, m), 9.73 (2H, d, $J$ = 3.4 Hz); $\delta_C$ (75 MHz; DMSO-$d_6$; $Me_4Si$; 25 °C) 20.9 (C27), 30.6, 30.7, 35.7, 62.4, 62.8, 65.1, 71.0, 120.9, 122.0, 124.9, 125.0, 125.8, 127.2, 127.6, 128.1, 128.2, 128.5, 128.6, 129.6, 130.0, 132.7, 133.0, 133.8, 135.5, 138.2, 138.3, 138.9, 139.0, 140.2, 140.5, 144.0, 145.7, 147.7, 151.7, 151.9, 152.3, 154.5, 155.9, 157.5, 157.9, 162.2; *m*/*z* (ESI-MS, API 3000) 262.6 ($M^{6+}$ requires 262.4), 343.9 ($[M + PF_6]^{5+}$ requires 344.8), 466.5 ($[M + 2PF_6]^{4+}$ requires 466.1), 670.2 ($[M + 3PF_6]^{3+}$ requires 669.8), 1077.4 ($[M + 4PF_6]^{2+}$ requires 1077.1).

**[(*Tolyl*Terpy)Ru(*L1*)]·(PF$_6$)$_3$ (*Ru1*·(PF$_6$)$_3$).** *Ru1*·$(PF_6)_3$ was synthesized from *Tolyl*TerpyRuCl$_3$ (26.6 mg, $5 \times 10^{-2}$ mmol) and *L1*·Br (63.7 mg, $5 \times 10^{-2}$ mmol) following the procedure described for the synthesis of *Ru3A*·$(PF_6)_9$, in 71% yield (Found: C, 46.8; H, 3.1; F, 27.1; N, 7.4; P, 7.5; Ru, 7.6. $C_{50}H_{40}F_{18}N_7P_3Ru$ requires C, 47.1; H, 3.2; F, 26.8; N, 7.7; P, 7.3; Ru, 7.9%); $\delta_H$ (300 MHz; DMSO-$d_6$; $Me_4Si$; 25 °C) 2.53 (6H, s, $H_{30}$ and $H_{17}$), 5.95 (2H, br s, $H_{12}$), 7.25 (2H, t, $^3J$ = 6.6 Hz, $H_{21}$), 7.33–7.38 (4H, m, $H_{15}$ and $H_3$), 7.48 (2H, d, $^3J$ = 5.4 Hz, $H_{14}$), 7.55–7.61 (6H, m, $H_{28}$, $H_4$ and $H_{11}$), 8.08 (2H, t, $^3J$ = 7.7 Hz, $H_{20}$), 8.15 (2H, t, $^3J$ = 7.7 Hz, $H_2$), 8.39 (2H, d, $^3J$ = 8.1 Hz, $H_{27}$), 9.07 (2H, d, $^3J$ = 8.1 Hz, $H_1$), 9.12–9.15 (4H, m, $H_{10}$ and $H_{19}$), 9.50 (2H, s, $H_{24}$ or $H_7$), 9.60 (2H, d, $^3J$ = 6.2 Hz, $H_{18}$), 9.71 (2H, s, $H_{24}$ or $H_7$); $\delta_C$ (75 MHz; DMSO-$d_6$; $Me_4Si$; 25 °C) 21.2 ($C_{17}$), 21.4 ($C_{30}$), 63.6 ($C_{12}$), 121.4 ($C_{24}$ or $C_7$), 122.5 ($C_{24}$ or $C_7$), 125.3 ($C_1$), 125.4 ($C_{10}$ or $C_{19}$), 126.3 ($C_{10}$ or $C_{19}$), 128.1 ($C_{27}$ and $C_{21}$), 128.6 ($C_3$ or $C_{15}$), 129.2 ($C_4$, $C_{28}$ or $C_{11}$), 130.4 ($C_3$ or $C_{15}$), 130.5 ($C_4$, $C_{28}$ or $C_{11}$), 131.9 ($C_{13}$), 133.5 ($C_{23}$ or $C_6$), 138.7 ($C_2$), 138.8 ($C_{20}$), 139.5 ($C_{16}$), 139.6 ($C_{29}$), 141.0 ($C_{22}$), 146.0 ($C_{18}$), 148.2 ($C_{26}$), 152.2 ($C_{23}$ or $C_6$), 152.7 ($C_{14}$), 152.8 ($C_4$, $C_{28}$ or $C_{11}$), 155.0 ($C_9$), 156.4 ($C_5$), 157.9 ($C_{25}$), 158.4 ($C_8$); *m*/*z* (ESI-MS, API 3000) 280.9 ($M^{3+}$ requires 280.0), 492.5 ($[M + PF_6]^{2+}$ requires 492.5), 1130.4 ($[M + 2PF_6]^{+}$ requires 1129.9).

## Acknowledgements

M. Bourbin and N. Boccon, both students from the Ecole Nationale Supérieure de Chimie de Paris, are strongly acknowledged for their participation in the electrochemical and spectroscopic measurements during their training period in the PPSM laboratory.

## References

1 J. G. Vos and J. M. Kelly, *Dalton Trans.*, 2006, 4869–4883.
2 C. Kaes, A. Katz and M. W. Hosseini, *Chem. Rev.*, 2000, **100**, 3553–3590.
3 E. C. Constable, *Chem. Soc. Rev.*, 2007, **36**, 246–253.
4 H. Hofmeier and U. S. Schubert, *Chem. Soc. Rev.*, 2004, **33**, 373–399.
5 P. R. Andres and U. S. Schubert, *Adv. Mater.*, 2004, **16**, 1043–1068.
6 J. P. Sauvage, J. P. Collin, J. C. Chambron, S. Guillerez, C. Coudret, V. Balzani, F. Barigelletti, L. D. Cola and L. Flamigni, *Chem. Rev.*, 1994, **94**, 993–1019.
7 E. Baranoff, J.-P. Collin, L. Flamigni and J.-P. Sauvage, *Chem. Soc. Rev.*, 2004, **33**, 147–155.
8 E. Figgemeier, L. Merz, B. A. Hermann, Y. C. Zimmermann, C. E. Housecroft, H. J. Guntherodt and E. C. Constable, *J. Phys. Chem. B*, 2003, **107**, 1157–1162.
9 E. C. Constable, E. L. Dunphy, C. E. Housecroft, W. Kylberg, M. Neuburger, S. Schaffner, E. R. Schofield and C. B. Smith, *Chem. Eur. J.*, 2006, **12**, 4600–4610, and references therein.
10 C. R. Mayer, E. Dumas, A. Michel and F. Secheresse, *Chem. Commun.*, 2006, 4183–4185.
11 E. C. Constable, C. E. Housecroft, M. Neuburger, D. Phillips, P. R. Raithby, E. Schofield, E. Sparr, D. A. Tocher, M. Zehnder and Y. Zimmermann, *J. Chem. Soc., Dalton Trans.*, 2000, 2219–2228.
12 E. C. Constable, *Chem. Commun.*, 1998, 403–404.
13 D. G. Kurth, J. P. Lopez and W.-F. Dong, *Chem. Commun.*, 2005, 2119–2121.

14 C. R. Mayer, E. Dumas and F. Secheresse, *Chem. Commun.*, 2005, 345–347.
15 C. R. Mayer, E. Dumas, F. Miomandre, R. Meallet-Renault, F. Warmont, J. Vigneron, R. Pansu, A. Etcheberry and F. Secheresse, *New J. Chem.*, 2006, **30**, 1628–1637.
16 W.-L. Jia, Y.-F. Hu, J. Gao and S. Wang, *Dalton Trans.*, 2006, 1721–1728.
17 P. Belser, A. v. Zelewsky, M. Frank, C. Seel, F. Vogtle, L. D. Cola, F. Barigelletti and V. Balzani, *J. Am. Chem. Soc.*, 1993, **115**, 4076–4086.
18 J. M. D. Wolf, R. Hage, J. G. Haasnoot, J. Reedijk and J. G. Vos, *New J. Chem.*, 1991, **15**, 501–507.
19 K. Onitsuka, N. Ohara, F. Takei and S. Takahashi, *Dalton Trans.*, 2006, 3693–3698.
20 P. U. Maheswari, B. Modec, A. Pevec, B. Kozlevcar, C. Massera, P. Gamez and J. Reedijk, *Inorg. Chem.*, 2006, **45**, 6637–6645.
21 A. Juris, V. Balzani, F. Barigelletti, S. Campagna, P. Belser and A. von Zelewsky, *Coord. Chem. Rev.*, 1988, **84**, 85–277.
22 E. C. Constable, E. Figgemeier, C. E. Housecroft, J. Olsson and Y. C. Zimmermann, *Dalton Trans.*, 2004, 1918–1927.
23 R. J. Gale and R. A. Osteryoung, *J. Electrochem. Soc.*, 1980, **127**, 2167–2172.
24 L. M. Vrana and K. J. Brewer, *J. Photochem. Photobiol., A*, 1997, **109**, 201–211.
25 A. J. Bard and L. R. Faulkner, *Electrochemical Methods: Fundamentals and Applications*, John Wiley and Sons Inc., New York, 2001, ch. 6.
26 M. Sharp, *Electrochim. Acta*, 1983, **28**, 301–308.
27 E. C. Constable, C. E. Housecroft, E. R. Schofield, S. Encinas, N. Armaroli, F. Barigelletti, L. Flamigni, E. Figgemeier and J. G. Vos, *Chem. Commun.*, 1999, 869–870.
28 E. C. Constable and A. M. W. C. Thompson, *J. Chem. Soc., Dalton Trans.*, 1992, 2947–2950.
29 S. S. Elmorsy, A. Pelter and K. Smith, *Tetrahedron Lett.*, 1991, **32**, 4175–4176.
30 Q. He, H. Huang, J. Yang, H. Lin and F. Bai, *J. Mater. Chem.*, 2003, **13**, 1085–1089.
31 J. P. Collin, S. Guillerez, J. P. Sauvage, F. Barigelletti, L. D. Cola, L. Flamigni and V. Balzani, *Inorg. Chem.*, 1991, **30**, 4230–4238.



 